

Short Communication:**Fabrication of Chitosan/Fe₃O₄ Nanocomposite as Adsorbent for Reduction Methylene Blue Contents**La Harimu^{1*}, Sri Wahyuni¹, Nasrudin Nasrudin¹, Muhamad Jalil Baari², and Dian Permana²¹Department of Chemistry Education, Faculty of Teacher Training and Education, Universitas Halu Oleo, Jl. Kampus Hijau Bumi Tridharma, Anduonou, Kendari 93132, Indonesia²Department of Chemistry, Faculty of Science and Technology, Universitas Sembilanbelas November Kolaka, Jl. Pemuda, Kolaka 93511, Indonesia*** Corresponding author:**

email: harim_l@yahoo.co.id

Received: April 22, 2021

Accepted: March 2, 2022

DOI: 10.22146/ijc.65430

Abstract: Methylene blue (MB) is a dye in wastewater from textile industries that pollutes the water environment. Reduction of its content is necessary for protecting humans and the surrounding environment. This study fabricated chitosan/Fe₃O₄ nanocomposite through the mixture of chitosan from crab shell waste and magnetite (Fe₃O₄) from local sand iron with sodium tripolyphosphate (STPP)-sulfate crosslinker as an adsorbent to reduce methylene blue content. The obtained composite was characterized by Fourier Transform Infrared (FTIR) Spectrophotometer and X-Ray Diffraction (XRD) instrument. The contents of methylene blue before and after applying adsorbent-based nanocomposite were determined using an ultraviolet-visible (UV-Vis) spectrophotometer. FTIR characterization results show that chitosan and chitosan/Fe₃O₄ nanocomposite had successfully synthesized based on the typical vibrational peaks. The deacetylation degree of chitosan was 69.79%. Fe₃O₄ and chitosan/Fe₃O₄ nanocomposite, were confirmed by XRD patterns. The chitosan/Fe₃O₄ nanocomposite adsorption capacity reached 45.37 mg/g when adsorption occurred with 20 mg adsorbent, pH 9, and contact time of 1.5 h. Hence, the chitosan/Fe₃O₄ nanocomposite in this study has potency and is applicable to adsorb MB effectively.

Keywords: adsorption; adsorbent; chitosan-magnetite nanocomposite; methylene blue

■ INTRODUCTION

The textile, paper, and plastic industries have been developing every year. These developments generate many advantages for the people. However, it is also followed by the bad impacts from dye wastewater that is very dangerous for water or marine environments. An example of a dye substance with various applications in chemistry, the textile industry, and medicine is methylene blue (MB) [1]. MB is an organic compound containing heterocyclic and aromatic groups with the chemical formula C₁₆H₁₈N₃SCl. The excess content of MB in wastewater is hazardous because it is difficult to biodegrade, poisonous, and carcinogenic substances for humans who consume fish and other water/marine animals in the

contaminated area [2-3]. Moreover, the photosynthesis process of water plants is hindered, disturbs environmental esthetic, and decreases the level of ecological hygiene [4-5]. Thereby, the reduction or elimination of MB content from wastewater is important.

Several methods have been conducted to treat the dye wastewater problem. The adsorption method utilizing adsorbent substances is an effective and efficient way [6-8]. Polymer and pore materials are general adsorbents to adsorb dye waste in the wastewater, including methylene blue, which is chosen due to its effectiveness, abundance, and low price reasons [9-11]. An example of a biopolymer that has potency as a dye adsorbent is a chitosan [12-13]. Chitosan is a chitin derivative with a pore structure [14].

It is usually used as an adsorbent for heavy metals and dye waste based on its capability to attract metal ions or dye molecules. Protonated amine and hydroxyl groups are the centers of reactions between chitosan and other substances. These groups will interact with dye compounds by proton exchanges and/or coordination bonding formation [15]. However, chitosan is prone to coagulation, poor mechanical strength, and soluble in acid solution, thus limiting its usefulness as an adsorbent [16-17].

A combination of chitosan and magnetite (Fe_3O_4) forms chitosan/ Fe_3O_4 composite to cover the weakness of chitosan and increase the performance of chitosan as an adsorbent. This composite also improves chitosan stability, resistance to oxidation, and resistance to form aggregation [18]. Coating magnetite with polymers can increase the polymer functionalities and increase the performance of a polymer in many applications. Besides that, the magnetic property of resulted composite makes it easier to be separated and recovered from the solution by another magnetic field [5].

Previous research informed the effectiveness of methyl orange dye removal using chitosan/ Fe_3O_4 composite-based adsorbent [5]. In addition, chitosan/ Fe_3O_4 composite was also effective to adsorb heavy metals, for instance, Pb(II) and Ni(II) [19]. Then, removal of mercury content was effectively conducted using magnetic chitosan, which was cross-linked with glutaraldehyde [15]. Meanwhile, chitosan/ Fe_3O_4 composite is generally synthesized from commercial substances, for instance, FeCl_3 , FeSO_4 , or Fe(III) acetylacetonate with commercial chitosan, but it is known to have an expensive cost. Therefore, in this study, magnetite (Fe_3O_4) was obtained from local iron sand, and chitosan was synthesized by self from crab shell waste to produce chitosan/ Fe_3O_4 nanocomposite with sodium tripolyphosphate (STPP) as a crosslinker to generate methylene blue adsorbent. Then, it is continued by investigating the optimum condition of chitosan/ Fe_3O_4 nanocomposite to adsorb methylene blue through adsorption capacity.

■ EXPERIMENTAL SECTION

Materials

Crab shell waste was obtained from Pajala Village,

Southeast Sulawesi. Local iron sand was taken from Laea Village, Southeast Sulawesi. The dried iron sand was separated from impurities using a permanent magnet. Then, chemical reagents consist of NaOH (Merck), HCl 37% (Merck), NaOCl (Merck), glacial acetic acid (Merck), nitric acid (Merck), ammonium hydroxide (Merck), methylene blue, sodium tripolyphosphate (STPP) (Merck), and Na_2SO_4 (Merck).

Instrumentation

Functional groups of chitosan and chitosan/ Fe_3O_4 nanocomposite were characterized by FTIR ALPHA Bruker spectrophotometer with KBr pellet. Then, crystal lattices of Fe_3O_4 and chitosan/ Fe_3O_4 nanocomposite were analyzed by Bruker Advance X-ray diffractometer. Meanwhile, the contents of methylene blue after treatments toward the mixture of adsorbent-methylene blue in various pH, contact time, and adsorbent mass were measured by a UV-Visible HITACHI U-2900 spectrophotometer at a wavelength of 664 nm.

Procedure

Isolation of Fe_3O_4 from local sand iron

Isolation of Fe_3O_4 from local sand iron was modified from Rahmi et al. [15]. Local sand iron was sieved by 100 mesh sieve. The sieved sand iron (30 g) was mixed into 100 mL HCl 37%. This mixture was heated at 70 °C for 1 h under stirred. Then, the residue was filtered and separated from the filtrate. The obtained filtrate was added slowly by NH_4OH (25%) solution under heated at 70 °C for 1 h until a black solid formed. This solid was neutralized by deionized water and dried in the oven at 105 °C.

Synthesis of chitosan from crab shell

Crab shell waste was washed with water, dried, ground, and sieved by a 100 mesh sieve tool to obtain powder form. Isolation steps of chitin consisted of deproteination (protein elimination), demineralization (minerals elimination), and depigmentation (pigment elimination). The Deproteinination step was carried out by weighing 200 mg of crab shell powder. Then it was reacted to NaOH (5%) solution at a ratio of 1:10 and heated for 2 h at 80 °C under stirring. After that, the

deposit was filtered, neutralized with deionized water until reached pH 7, and dried at 80 °C for 24 h.

Demineralization step was carried out by reaction of protein-free chitin and HCl (1.5 M) solution at a ratio of 1:10 under heating at 80 °C and stirring for 2 h. The deposit was filtered, neutralized with deionized water until reached pH 7, and dried at 80 °C for 24 h.

In the depigmentation step, chitin with fixed weight was reacted to NaOCl (0.5%) solution at a ratio of 1:10 and heated for 2 h at 80 °C under stirring. Then, the solid was filtered, neutralized with deionized water, and dried at 80 °C for 24 h.

Furthermore, chitin was deacetylated to synthesize chitosan through a chemical reaction between chitin and NaOH (50%) solution at a ratio of 1:10 and heated for 2 h at 80 °C under stirring. After that, the solid was filtered, neutralized with deionized water, and dried at 80 °C for 24 h. Functional groups of synthesized chitosan were characterized with an FTIR spectrophotometer. IR spectra were also used to analyze the percent of deacetylation degree (%DD) based on the baseline method, which applies Eq. (1) as follows [20].

$$\%DD = 1 - \left[\frac{A_{1655}}{A_{3450}} \times \frac{1}{1.33} \right] \times 100\% \quad (1)$$

Preparation of chitosan-Fe₃O₄ nanocomposite

Synthesis of chitosan-Fe₃O₄ nanocomposite was carried out by modification of Udoetok et al. and Wulandari et al. methods [21-22]. Chitosan (1.25 g) was dissolved into 250 mL acetic acid 1% solution (v/v) to obtain chitosan solution 0.5% (w/v). Meanwhile, Fe₃O₄ was suspended in 250 mL of deionized water. Then, 50 mL from each solution and suspension were mixed to form a ferrogel solution. This mixture was stirred using a magnetic stirrer for 30 min. Ferrogel solution was cross-linked with the addition of 50 mL STPP-sulfate crosslinker at the ratio of 5:1 via syringe pump (dropping rate 20 mL/h) under stirring. Chitosan/Fe₃O₄ in the colloid form was neutralized and suspended by 50 mL of deionized water. After that, it was stored in the refrigerator at 4 °C. The composite was characterized with an X-ray diffractometer and FTIR spectrophotometer.

Optimization of adsorption parameters

Determination of optimum pH. The chitosan/Fe₃O₄ nanocomposite (20 mg) was entered into 10 mL of methylene blue solution (100 mg/L) at pH 2. The beaker glass was covered with aluminum foil and stirred with a magnetic stirrer for 30 min. After that, it was filtered using Whatman 42 grade filter paper. Similar treatments were repeated for pH 5, 7, and 9. The content of methylene blue in this filtrate was measured with a UV-Visible spectrophotometer at a wavelength of 664 nm.

Determination of optimum contact time. The chitosan/Fe₃O₄ nanocomposite (20 mg) was entered into 10 mL of methylene blue solution (100 mg/L) at the optimum pH. The beaker glass was covered with wrapping plastic stirred with a magnetic stirrer for 0.5, 1.0, 1.5, and 2.0 h, respectively. Then, the adsorbent was separated from the solution by Whatman 42 grade filter paper. The content of methylene blue in this filtrate was measured by a UV-Visible spectrophotometer at a wavelength of 664 nm.

Determination of optimum mass. The optimum mass of nanocomposite as methylene blue adsorbent was determined by preparing various masses of nanocomposite from 20, 40, 60, and 80 mg. Each variant was mixed with 10 mL methylene blue solution (100 mg/L) using the optimum pH. The Beaker glass was covered with wrapping plastic stirred with a magnetic stirrer by applying optimum contact time. Then, the adsorbent was separated from the solution by Whatman 42 grade filter paper. The content of methylene blue in this filtrate was measured by a UV-Visible spectrophotometer at a wavelength of 664 nm.

The concentration of adsorbed methylene blue was obtained by subtracting the initial concentration from the remaining concentration. This remaining concentration was determined through the equation from the standard regression curve that plots absorbance and concentration. The concentration of adsorbed methylene blue by the presence of chitosan/Fe₃O₄ nanocomposite was calculated by Eq. (2).

$$[MB]_{ads} = [MB]_{initial} - [MB]_{final} \quad (2)$$

Adsorbed methylene blue content or the adsorption capacity, Q (mg/g) of chitosan/ Fe_3O_4 nanocomposite was calculated by Eq. (3) [1]:

$$Q = \frac{[\text{MB}]_{\text{initial}} - [\text{MB}]_{\text{final}}}{m_{\text{ads}}} \times V_{\text{sol}} \quad (3)$$

where $[\text{MB}]_{\text{ads}}$ is the concentration of adsorbed MB, $[\text{MB}]_{\text{initial}}$ is the initial concentration of MB (mg/L), $[\text{MB}]_{\text{final}}$ is the concentration of MB at equilibrium (mg/L), m_{ads} is adsorbent mass (g), and V_{sol} is the volume of MB solution (L).

■ RESULTS AND DISCUSSION

Isolation of Chitin and Synthesis of Chitosan

The obtained chitosan powder was yellowish-white. The deacetylation degree (DD) of chitosan was determined by the Domszy and Robert baseline method. Analysis results showed that the DD value reached 69.79%. Therefore, the obtained compound could be categorized as chitosan. Then, it was characterized by an FTIR spectrophotometer to confirm the specific functional groups.

Meanwhile, the compliance of synthesized chitosan and commercial/standard chitosan is listed in Table 1, which relates the vibrational type of functional group and its wavenumber. The results in Table 1 show the similarity of absorption spectra between synthesized chitosan and commercial/standard chitosan. Thereby, chitosan has successfully been produced. The difference may lie in the deacetylation degree (DD) and molecular weight of each chitosan.

The Isolation of Fe_3O_4 from Local Iron Sand and Synthesis of Chitosan/ Fe_3O_4 Nanocomposite

Isolation of Fe_3O_4 compound from 30 g of local iron sand produced 8.6386 g Fe_3O_4 or has a yield of 28.8%. Then, chitosan/ Fe_3O_4 nanocomposite was synthesized via cross-linking reaction with STPP-sulfate as a crosslinker. The two materials were analyzed using an X-ray diffractometer. The diffractograms of isolated Fe_3O_4 and chitosan/ Fe_3O_4 nanocomposite are displayed in Fig. 1.

The XRD pattern of isolated Fe_3O_4 from local iron sand generated similar peaks with the XRD pattern of the Fe_3O_4 standard according to the standard data of Fe_3O_4 -ICSD#26410. This is proved based on four characteristic peaks at $2\theta = 30.205^\circ$, 35.515° , 43.325° , and 53.711° respectively, with the lattice plane at (220), (311), (400), and (422) in the diffractogram. A broad peak at $2\theta = 35.515^\circ$ corresponds to the nature and small crystal of the isolated Fe_3O_4 [23]. Besides that, there are other peaks with a lower intensity which are thought to be maghemite ($\gamma\text{-Fe}_2\text{O}_3$) based on the standard $\text{Fe}_2\text{O}_3(\text{gamma})$ -ICSD#172905. Meanwhile, for the diffractogram of the nanocomposite, the relatively low peak intensity corresponds to the crystallinity of chitosan that reduces after cross-linking reactions [15]. Consequently, this amorphous structure can increase the accessibility of methylene blue to be adsorbed on the nanocomposite via active sites [15]. A low-intensity peak at $2\theta = 21^\circ$ relates to the peak character of chitosan. The average size of the Fe_3O_4 and chitosan/ Fe_3O_4

Table 1. The comparison of wavenumber values from vibrational peaks of the functional group on FTIR spectra between synthesized chitosan and commercial/standard chitosan

Functional group (vibration type)	Commercial chitosan wavenumber (cm^{-1})	Synthesized chitosan wavenumber (cm^{-1})
N-H (stretching)	3442	3428
C-H aliphatic (stretching)	2883	2878
C=O amide I (stretching)	1651	1655
N-H amide II (bending)	1593	1597
C-N (stretching)	1421	1423
CH_3 sym (bending)	1377	1381
C-O-C in cyclic (stretching)	1251	1260
C-O-C (stretching)	1153	1155
C-OH (stretching)	1033	1086

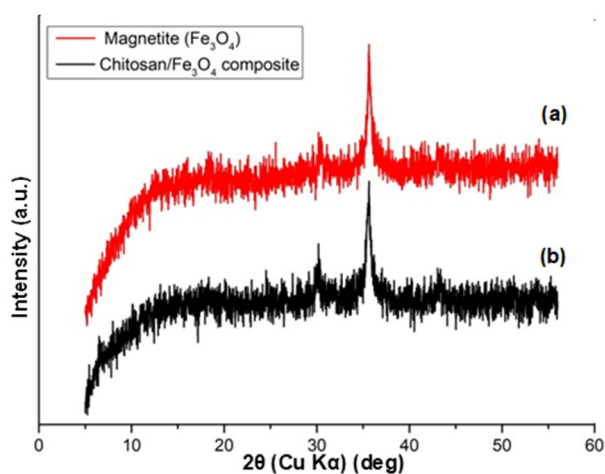


Fig 1. The diffractogram of (a) isolated Fe_3O_4 from local iron sand and (b) chitosan/ Fe_3O_4 nanocomposite

nanocomposite crystal (D) was calculated using the Scherrer formula based on all diffraction peaks. This is displayed in Eq. (4) [24].

$$D = \frac{K\lambda}{\beta \cos\left(\frac{2\theta}{2}\right)} \quad (4)$$

where K is constant ($K = 0.94$), which is a correction factor to determine the full width half maximum (FWHM), λ is the applied wavelength of the copper source (1.54056 \AA), β is the FWHM of the diffraction peak, θ is diffraction angle, and $\cos \frac{2\theta}{2}$ is the cosine of the angle where the diffraction peak was observed. The calculated results inform that the crystal sizes of Fe_3O_4 from local sand iron and chitosan- Fe_3O_4 composite are 3.683 and 3.108 nm, respectively. Therefore, isolated Fe_3O_4 and chitosan-magnetite composite are classified as nanomaterials.

Meanwhile, the information of IR spectra from obtained chitosan/ Fe_3O_4 composite are listed in Table 2. Specific functional groups contained in this composite are confirmed based on bonding vibrations among atoms.

Table 2 displays several vibrational peaks from composite functional groups that shift after forming a composite. The typical absorption peak at wavelengths 3389 cm^{-1} relates to $-\text{O}-\text{H}$ and $-\text{N}-\text{H}$ stretching vibrations. Then, the absorption peak at 2922 cm^{-1} corresponds to stretching vibrations of $-\text{C}-\text{H}$ aliphatic. Furthermore, the vibrational peaks at 1655 cm^{-1} , 1597 cm^{-1} , and 1423 cm^{-1} from $-\text{C}=\text{O}$ amide I, $-\text{N}-\text{H}$ acetamide, and $-\text{C}-\text{N}$ bonds

Table 2. The wavenumber values from vibrational peaks of the functional group on FTIR spectra of chitosan/ Fe_3O_4 nanocomposite

Functional group (vibration type)	Wavenumber (cm^{-1})
N-H (stretching)	3389
C-H aliphatic (stretching)	2922
C=O amide I (stretching)	1616
N-H amide II (bending)	1528
C-N (stretching)	1415
CH_3 sym (bending)	1395
C-O-C in cyclic (stretching)	1100-1020
Fe-O (bending)	1072
Fe-O (stretching)	573
Fe-O (stretching)	442

respectively in chitosan IR spectra shift to lower wavenumber. This corresponds to the stiffness of molecular vibration due to the linkage of phosphoric and ammonium ions in acetamide groups. Peaks at 1100 up to 1020 cm^{-1} relate to $-\text{C}-\text{O}$ stretching vibrations. Meanwhile, the presence of Fe-O bond was confirmed from the absorption peaks at wavenumbers 573 cm^{-1} and 442 cm^{-1} [25]. Meanwhile, the bending vibration of Fe-O appears in 1072 cm^{-1} .

Optimum pH of Methylene Blue Adsorption by Chitosan/ Fe_3O_4 Nanocomposite

The performance of chitosan/ Fe_3O_4 nanocomposite is affected by the pH value of the system. This parameter is an important parameter during the process of dye adsorption [26]. The adsorption capacity of chitosan-magnetite nanocomposite as MB adsorbent at various pH is shown in Fig. 2.

Optimum performance of chitosan/ Fe_3O_4 nanocomposite as methylene blue adsorbent occurs at pH 9 with the adsorption capacity of 40.27 mg/g. This corresponds to the addition of a negative charge on the adsorbent surface, which generates more electrostatic interactions between active sites in adsorbent and methylene blue [27]. Chemical bonds can also be formed if there is sufficient energy. Whereas at lower pH, the adsorption of methylene blue is not optimal, and the number of electrostatic interactions and/or chemical bonds is reduced because the active groups on the

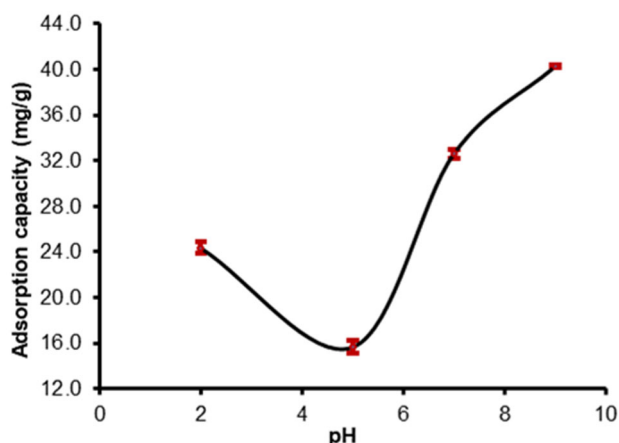


Fig 2. Correlation graphic between pH and adsorption capacity

adsorbent tend to be protonated by increasing hydrogen ions in solution. Consequently, a repulsive force dominates interactions among the active sites of the adsorbent and the methylene blue, which has a positive charge. A significant decrease in adsorption efficiency and adsorption capacity at pH 5 probably causes some active sites to be not protonated, but there is competition between hydrogen ions and MB molecules to adhere/bind on those active sites.

Determination of Optimum Contact Time

Determination of optimum contact time is required for information about the effectiveness and the durability of the chitosan/Fe₃O₄ nanocomposite to adsorb methylene blue. The adsorption capacity of the chitosan-magnetite nanocomposite as an adsorbent to reduce methylene blue concentration in the various contact times is displayed in Fig. 3.

The graph in Fig. 3 shows that the contact time affects the amount of adsorbed methylene blue. Initially, the amount of adsorbed methylene blue was still relatively small. This relates to the amount of methylene blue that is not much attached to active groups and pores of the chitosan/Fe₃O₄ nanocomposite. Contact time and pH value for supporting the optimum performance of chitosan/Fe₃O₄ nanocomposite are at 90 min and pH 9, respectively. The adsorption capacity increases when the contact time increases from 30 to 90 min. It indicates that the methylene blue molecule is still spreading and entering the active surface sites of chitosan/Fe₃O₄ nanocomposite

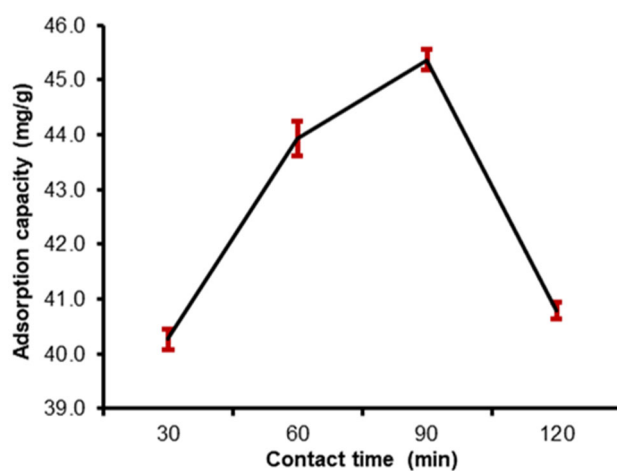


Fig 3. Correlation graphic between contact time and adsorption capacity

at this time range [28]. However, after 90 min, the performance of chitosan/Fe₃O₄ nanocomposite against methylene blue decreases due to equilibrium conditions in adsorption-desorption processes [29]. It also explains that MB probably forms a monolayer on the composite surface. The amount of methylene blue that is weakly adsorbed may return to desorb due to the stirring/shaking effect [30].

Determination of Optimum Adsorbent Mass

The effect of mass toward adsorption capacity of the chitosan/Fe₃O₄ nanocomposite as an adsorbent to reduce methylene blue concentration is displayed in Fig. 4.

Fig. 4 shows an increment and decrement in methylene blue absorption by the presence of chitosan/Fe₃O₄ nanocomposite at several masses. The addition of adsorbent mass from 30 to 40 mg increases the adsorption of methylene blue because the abundance of active sites and adsorbent pores also increases [31]. Optimum adsorption capacity occurs when the adsorption mass is 20 mg. All active groups and pores of adsorbent have pulled and bound methylene blue molecules optimally in this condition. Then, the decrease in adsorption capability at larger mass happens as a consequence large amount of hydrogen bond formation between active groups (amine and carboxylates) on the chitosan surface and also between active sites and water molecules in solution [5,7,29].

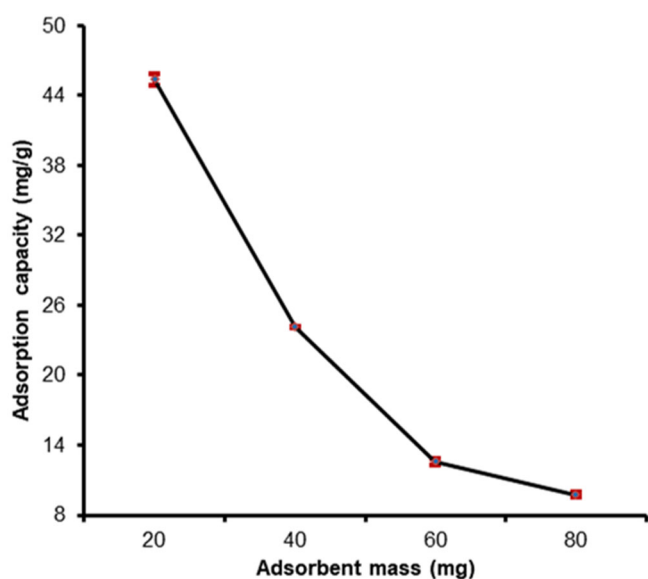


Fig 4. Correlation graphic between adsorbent mass and adsorption capacity

Therefore, the interaction of those active sites and MB molecules is restricted. Besides that, the increasing of adsorbent mass will increase the viscosity of the methylene blue solution so that ion movement in the solution is slowed. As a result, the amount of methylene blue with a larger molecular weight that must be adsorbed on the surface even reduces [30]. The maximum adsorption capacity reaches 45.37 mg/g. These results are different than the previous study in that adsorption efficiency, and adsorption capacity are 63.6% and 700 mg/g [3].

■ CONCLUSION

The use of local sand iron as a source of magnetite can be conducted through the isolation process. This magnetite compound can be combined with chitosan with plentiful specific functional groups to form chitosan/Fe₃O₄ nanocomposite. This composite was effective as an adsorbent for reducing methylene blue content. The largest adsorption capacity reached 45.37 mg/g. Optimum conditions, such as adsorbent mass, contact time, and pH of a system to support the performance of chitosan/Fe₃O₄ nanocomposite were 20 mg, 90 min, pH 9, respectively.

■ REFERENCES

[1] Pathania, D., Sharma, S., and Singh, P., 2017, Removal

of methylene blue by adsorption onto activated carbon developed from *Ficus carica* bast, *Arabian J. Chem.*, 10, S1445–S1451.

- [2] Pandey, S., Do, J.Y., Kim, J., and Kang, M., 2020, Fast and highly efficient removal of dye from aqueous solution using natural locust bean gum based hydrogels as adsorbent, *Int. J. Biol. Macromol.*, 143, 60–75.
- [3] Ishmaturrehmi, I., Rahmi, R., and Mustafa, I., 2019, The influence of Fe₃O₄ on magnetic chitosan composite preparation for methylene blue removal from water, *IOP Conf. Ser.: Mater. Sci. Eng.*, 523, 012020.
- [4] Vezentsev, A.I., Thuy, D.M., Goldovskaya-Peristaya, L.F., and Glukhareva, N.A., 2018, Adsorption of methylene blue on the composite sorbent based on bentonite-like clay and hydroxyapatite, *Indones. J. Chem.*, 18 (4), 733–741.
- [5] Haldorai, Y., Kharismadewi, D., Tuma, D., and Shim, J.J., 2015, Properties of chitosan/magnetite nanoparticles composites for efficient dye adsorption and antibacterial agent, *Korean J. Chem. Eng.*, 32 (8), 1688–1693.
- [6] Zhang, C., Dai, Y., Wu, Y., Lu, G., Cao, Z., Cheng, J., Wang, K., Yang, H., Xia, Y., Wen, X., Ma, W., Liu, C., and Wang, Z., 2020, Facile preparation of polyacrylamide/chitosan/Fe₃O₄ composite hydrogels for effective removal of methylene blue from aqueous solution, *Carbohydr. Polym.*, 234, 115882.
- [7] Harimu, L., Rudi, L., Haetami, A., Santoso, G.A.P., and Asriyanti, 2019, Studi variasi konsentrasi NaOH dan H₂SO₄ untuk memurnikan silika dari abu sekam padi sebagai adsorben ion logam Pb²⁺ dan Cu²⁺, *Indo. J. Chem. Res.*, 6 (2), 81–87.
- [8] Harimu, L., Haeruddin, Baari, M.J., and Sutapa, I.W., 2020, Effectiveness of reducing cyanide levels in the *Dioscorea hispida* Dennst bulbs through soaking in seawater and interaction with ash scrub, *J. Phys.: Conf. Ser.*, 1463, 012013.
- [9] Esmizadeh, E., Tanzifi, M., Bazgir, H., Nazari, A., and Vahidifar, A., 2019, Adsorption of methylene blue dye from aqueous solution using

- polyaniline/xanthan gum nanocomposite: kinetic and isotherm studies, *J. Polym. Compos.*, 7 (1), 17–26.
- [10] Nakamoto, K., and Kobayashi, T., 2017, Fibrous mordenite zeolite - polymer composite adsorbents to methylene blue dye, *Int. J. Eng. Res. Technol.*, 7 (12), 131–136.
- [11] Budnyak, T.M., Aminzadeh, S., Pylypchuk, I.V., Sternik, D., Tertykh, V.A., Lindström, M.E., and Sevastyanova, O., 2018, Methylene blue dye sorption by hybrid materials from technical lignins, *J. Environ. Chem. Eng.*, 6 (4), 4997–5007.
- [12] Bulut, Y., and Karaer, H., 2015, Adsorption of methylene blue from aqueous solution by cross-linked chitosan/bentonite composite, *J. Dispersion Sci. Technol.*, 36 (1), 61–67.
- [13] Kellner-Rogers, J.S., Taylor, J.K., Masud, A.M., Aich, N., and Pinto, A.H., 2019, Kinetic and thermodynamic study of methylene blue adsorption onto chitosan: Insights about metachromasy occurrence on wastewater remediation, *Energy Ecol. Environ.*, 4 (3), 85–102.
- [14] Zainol Abidin, N.A., Kormin, F., Zainol Abidin, N.A., Mohamed Anuar, N.A., and Abu Bakar, M.F., 2020, The potential of insects as alternative sources of chitin: An overview on the chemical method of extraction from various sources, *Int. J. Mol. Sci.*, 21 (14), 4978.
- [15] Rahmi, Fathurrahmi, Lelifajri, and PurnamaWati, F., 2019, Preparation of magnetic chitosan using local iron sand for mercury removal, *Heliyon*, 5 (5), e01731.
- [16] Dimonie, D., Dima, S.O., and Petrache, M., 2013, Influence of centrifugation on the molecular parameters of chitosan solubilized in weakly acidic aqueous solutions, *Dig. J. Nanomater. Biostruct.*, 8 (4), 1799–1809.
- [17] Szymańska, E., and Winnicka, K., 2015, Stability of chitosan - A challenge for pharmaceutical and biomedical applications, *Mar. Drugs*, 13 (4), 1819–1846.
- [18] Arami, H., Stephen, Z., Veiseh, O., and Zhang, M., 2011, "Chitosan-Coated Iron Oxide Nanoparticles for Molecular Imaging and Drug Delivery" in *Chitosan for Biomaterials I. Advances in Polymer Science*, Eds. Jayakumar, R., Prabakaran, M., and Muzzarelli, R., Springer, Berlin, Heidelberg, vol. 243, 163–184.
- [19] Tran, H.V., Tran, L.D., and Nguyen, T.N., 2010, Preparation of chitosan/magnetite composite beads and their application for removal of Pb(II) and Ni(II) from aqueous solution, *Mater. Sci. Eng., C*, 30 (2), 304–310.
- [20] Domszy, J.G., and Roberts, G.A.F., 1985, Evaluation of infrared spectroscopic techniques for analysing chitosan, *Makromol. Chem.*, 186 (8), 1671–1677.
- [21] Udoetok, I.A., Wilson, L.D., and Headley, J.V., 2016, Self-assembled and cross-linked animal and plant-based polysaccharides: chitosan–cellulose composites and their anion uptake properties, *ACS Appl. Mater. Interfaces*, 8 (48), 33197–33209.
- [22] Wulandari, I.O., Mardila, V.T., Santjojo, D.J.D.H., and Sabarudin, A., 2018, Preparation and characterization of chitosan-coated Fe₃O₄ nanoparticles using ex-situ co-precipitation method and tripolyphosphate/sulphate as dual crosslinkers, *IOP Conf. Ser.: Mater. Sci. Eng.*, 299, 012064.
- [23] Saranya, T., Parasuraman, K., Anbarasu, M., and Balamurugan, K., 2015, XRD, FTIR and SEM study of magnetite (Fe₃O₄) nanoparticles prepared by hydrothermal method, *Nano Vision*, 5 (4-6), 149–154.
- [24] Zepeda, A.M., Gonzalez, D., Heredia, L.G., Marquez, K., Perez, C., Pena, E., Flores, K., Valdes, C., Eubanks, T.M., Parsons, J.G., and Cantu, J., 2018, Removal of Cu²⁺ and Ni²⁺ from aqueous solution using SnO₂ nanomaterial effect of: pH, time, temperature, interfering cations, *Microchem. J.*, 141, 188–196.
- [25] Asgari, S., Fakhari, Z., and Berijani, S., 2014, Synthesis and characterization of Fe₃O₄ magnetic nanoparticles coated with carboxymethyl chitosan grafted sodium methacrylate, *J. Nanostruct.*, 4 (1), 55–63.
- [26] Monier, M., and Abdel-Latif, D.A., 2013, Modification and characterization of PET fibers for

- fast removal of Hg(II), Cu(II) and Co(II) metal ions from aqueous solutions, *J. Hazard. Mater.*, 250-251, 122-30.
- [27] Zhang, J., Zhang, Y., Lei, Y., and Pan, C., 2011, Photocatalytic and degradation mechanisms of anatase TiO₂: A HRTEM study, *Catal. Sci. Technol.*, 1 (2), 273-278.
- [28] Kuang, Y., Zhang, X., and Zhou, S., 2020, Adsorption of methylene blue in water onto activated carbon by surfactant modification, *water*, 12 (2), 587.
- [29] Jain, N., Dwivedi, M.K., and Waskle, A., 2016, Adsorption of methylene blue dye from industrial effluents using coal fly ash, *Int. J. Adv. Eng. Res. Sci.*, 3 (4), 9-16.
- [30] Harimu, L., Matsjeh, S., Siswanta, D., and Santosa, S.J., 2010, Separation of Fe(III), Cr(III), Cu(II), Ni(II), Co(II), and Pb(II) metal ions using poly(eugenyl oxyacetic acid) as an ion carrier by a liquid membrane transport method, *Indones. J. Chem.*, 10 (1), 69-74.
- [31] Boukhemkhem, A., and Rida, K., 2017, Improvement adsorption capacity of methylene blue onto modified Tamazert kaolin, *Adsorpt. Sci. Technol.*, 35 (9-10), 753-773.